CFD Simulation of Concap Tray Hydrodynamics

Mohammed Rahim Ostadzehi [1], Rahbar Rahimi[1], Taleb Zarei[*2] and Mortaza Zivdar[1]**
[1]Department of Chemical Engineering, University of Sistan and Baluchestan, Zahedan, Iran
[2]Department of Mechanical Engineering, University of Hormozgan,BandarAbbas, Iran
(Received 11 December 2012, Accepted 12 March 2013)

Abstract

This research includes both experimental and CFD investigation in the hydrodynamic behavior of a new type of column tray introduced as "Concap" tray. The proposed column tray is used in contactor columns especially in stripping columns. The hydrodynamics of this Concap tray is investigated in a 1.2m in diameter column. Using air-water system, the experiments were performed for different liquid and vapor loads at constant ambient temperature and pressure. The clear liquid height and total pressure drop were measured. The results were compared with the experimental data of a valve tray in the same column simulator rig. The total pressure drop and clear liquid height of Concap tray were similar to a valve tray, having equal 14% open holes area. Liquid velocity distribution on the tray has been predicted by CFD and is reported.

Keywords: CFD, Distillation, Concap tray, Valve tray, Hydrodynamics

Introduction

In recent years, many efforts have been done in order to improve the equipment and trays of distillation or gas-liquid contact devices, due to global requirements for a more sustainable process industry. Over the past years, the design of contactor devices have significantly changed in design to obtain better efficiency and lower pressure drops as well as to correct certain other deficiencies. For instance, weeping at low gas loads or entrainment at high gas loads that frequently encountered in commercial operation.

Concap tray utilizes a special cone aperture that adds pressure gradient driving force to the chemical potential gradient for enhancing mass transfer rates [1].Two general designs of trays or contacting devices and their modifications are used in recent applications, including sieve and valve trays which have their own merit [2].
In this research, a novel gas liquid contactor is introduced as Concaptray. The hydraulic of the Concap tray has been compared with valve tray in order to have an insight about the novel Concap tray.

The schematic diagram of Concap tray is shown in Fig. 1. The numbers illustrate different parts of the tray. The Concap tray is a flat perforated plate with risers around the holes, similar to a bubble cap tray, and open cones over the risers. Liquid and froth are trapped on the tray to a depth at least equal to the weir height or riser height. This enhances Concap tray ability to operate at low vapor and liquid rates as a bubble cap tray.

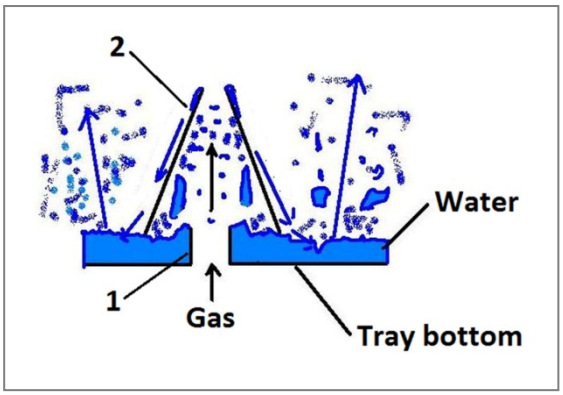

Figure 1: Schematic figure of Concap tray. The Concap tray is a flat perforated plate with risers around the holes (1)and open cones (2) over the risers.

Separation mechanism in this tray differs from conventional trays. The gas rises through the riser and the open cone. When gas passes through the open cone with a variable cross-section, based on the Bernoulli's law its velocity and kinetic energy will increase whilst its pressure will decrease. The pressure drop in the upper

* Corresponding author: Tel: +98-7617660042 Fax: +98-7617660032 Email: talebzarei@yahoo.com
** Unfortunately, the editorial office was informed that Mr. Mohammed Rahim Ostadzehi has just been passed away. With a great sadness and sorrow, a sincere condolence is forwarded to the other co-authors as well as his esteemed family. May Allah (s.w.) reward him in the dayafter.

part of the open cone leads to a suction in the lower part. Hence, light component in the liquid phase will desorb to the gas phase and stripping will take place. This mechanism corresponds with this fact "To make conditions more favorable for desorption or stripping the temperature may be increased or the total pressure reduced"[2]. This suction mechanism causes a high turbulence of the liquid on the tray. Therefore, the gas and light component of liquid efficiently separate. The suction and the contact of the gas with the liquid make a frothy or spray region on the tray. In addition, mass transfer operation is occurring in this region. The Concap tray can also operate at low liquid rate. These are major advantages of this kind of tray.

In recent years, there are considerable academic and industrial interests in the use of computational fluid dynamic (CFD) to model two-phase flows in some chemical engineering equipment. There have been many attempts to simulate sieve tray hydrodynamics using CFD. The interphase momentum exchange (drag) coefficient was required to model the hydrodynamics of multiphase flow on sieve tray. Gesit et al. [3] developed a 3-D CFD model to predict the flow patterns and hydraulics of commercial-scale sieve trays. Their geometry and operating conditions were based on experimental works of Solari and Bell [4] at a distillation tower 1.213m in diameter that has been done at Fractionation Research Inc. The predicted results were in good agreement with experimental results. Rahimi et al. [5] developed a three-dimensional, two-phase CFD model to determine the hydrodynamic and concentration distribution in both liquid and vapor phases at the sieve tray. In their work, the hydrodynamics, mass transfer and heat transfer of sieve tray were predicted and the point and tray efficiencies were determined by computational fluid dynamics. Li et al. [6] simulated the hydraulics of a full open valve tray using fluid dynamic modeling. Based on the clear liquid height measurement on a test valve tray, a new relationship for the liquid entrainment was developed and the momentum transfer term was calculated at the interface of gas and liquid. Zarei et al. [7] predicted the flow pattern and hydraulics of a MVG tray by using CFD simulation. They have reported less clear liquid height and pressure drop and more distribution rate for MVG tray compared with the sieve tray.

Nowadays, CFD is becoming a powerful research and an effective tool for understanding the complex hydrodynamics in chemical industrial equipment. Therefore, in this paper, a 3-D transient CFD model was developed for hydrodynamics of a 1.2 m in diameter Concap tray and the results were validated with experimental data and compared with a valve tray in similar conditions.

2. Experimental setup

The flow diagram of experimental setup is illustrated in Fig. 2. The column consists of two 1.2 m in diameter Concap trays and ancillary gas and liquid distribution devices. The column has three sight glasses to facilitate the observation of the phenomena that occurs in the column. The tray spacing is considered 0.61 m. In addition, a blower blows air up through the column. Water is pumped from a storage tank by means of a centrifugal pump into the column. The water flow rate is measured by the calibrated flow meter. The water is considered either to return to the tank or straight to drain. The air vents to surroundings.

To uniform and calm distribution of water, the upper sieve tray inlet down-comer filled with a pall rings. The down-comer area is 0.061608 m^2. The gas velocity was measured using a calibrated pitot tube at the blower outlet.

Constant weir height, down-comer clearance and tray spacing were used in the experiments. Dry tray pressure drop is measured by blocking off the clearance under the downcomers. The pressure drop of each tray is measured by the manometers that were connected to the pressure taps.

The pressure taps were positioned at 10cm under and at 40 cm above the tray. The clear liquid height is measured by subtracting the dry pressure drop from total pressure drop at fixed vapor superficial velocities [8].

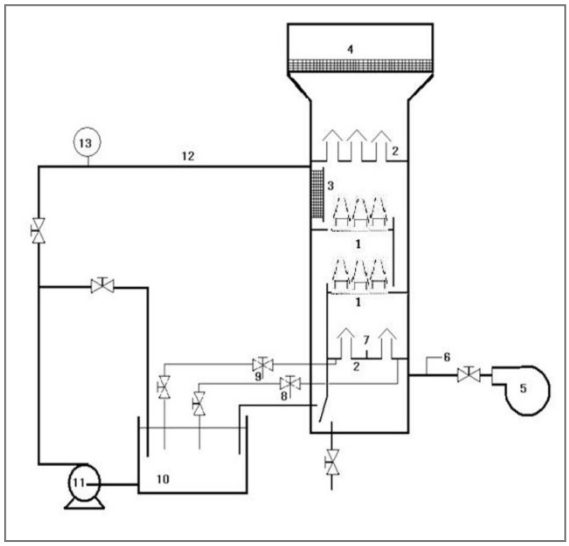

Figure 2: Schematic of experimental set-up to measure hydrodynamics of Concape tray. 1, Concap trays; 2, chimney trays; 3, downcomer filled with pall ring; 4, demister pad; 5, air blower; 6, pitot tube; 7, transverse baffle; 8, upstream weeping line; 9, downstream weeping line; 10, storage tank for liquid; 11, liquid pump; 12, inlet liquid line; 13, liquid flow meter [8].

3. Model equations

The dispersed gas and the continuous liquid have been modeled in the Eulerian-Eulerian frame work as two interpenetrating phases having separate transport equations. Thus, for each phase the time and volume averaged conservation equations were numerically solved. In this work, the energy and mass transfer have not been considered. The gas and liquid volume fractions, $\alpha_G$and α_L, are related by the summation constraint.

$$\alpha_G + \alpha_L = 1 \qquad (1)$$

Eqs.2 and 3 are continuity equations for gas and liquid phases. Where, ρ ,V and. α are density , velocity vector and volume fraction, respectively. In the following equations the subscripts G and L represent gas and liquid phases, respectively.

$$\frac{\partial(\alpha_G \rho_G)}{\partial t} + \nabla.(\alpha_G \rho_G V_G) = 0 \qquad (2)$$

$$\frac{\partial(\alpha_L \rho_L)}{\partial t} + \nabla.(\alpha_L \rho_L V_L) = 0 \qquad (3)$$

The gas and liquid phase momentum equations are;

$$\frac{\partial}{\partial t}(\alpha_G \rho_G V_G) + \nabla.(\alpha_G(\rho_G V_G V_G)) = -\alpha_G \nabla P_G + \nabla.(\alpha_G \mu_{eff,G}(\nabla V_G + (\nabla V_G)^T)) - M_{GL} \qquad (4)$$

$$\frac{\partial}{\partial t}(\alpha_L \rho_L V_L) + \nabla.(\alpha_L(\rho_L V_L V_L)) = -\alpha_L \nabla P_L + \nabla.(\alpha_L \mu_{eff,L}(\nabla V_L + (\nabla V_L)^T)) + M_{GL} \qquad (5)$$

The same pressure field was assumed for both phases, which is P_G=P_L.

The effective viscosities of the gas and liquid phases are $\mu_{eff,G}$ and $\mu_{eff,L}$,respectively.

$$\mu_{eff,G} = \mu_{Laminar,G} + \mu_{Turbulent,G} \qquad (6)$$

$$\mu_{eff,L} = \mu_{Laminar,L} + \mu_{Turbulent,L} \qquad (7)$$

The term M_{GL} in equations 4 and 5 describes the interfacial forces acting on each phase due to the presence of the other phase. The interphase momentum transfer term M_{GL} is basically the interphase drag force per unit volume. With the gas as the disperse phase, the equation for M_{GL} is:

$$M_{GL} = \frac{3}{4}\frac{C_D}{d_G}\alpha_G \rho_L |V_G - V_L|(V_G - V_L) \qquad (8)$$

Where d_G is mean bubble diameter and C_D is drag coefficient. Value of C_D for the case of distillation is not well known. However, Fischer and Quarini [9] assumed a constant value of 0.44. This value is appropriate for large bubbles of spherical cap shape and the turbulent fluid flow. Experimental observations showed that for the Concap tray the bubbles are large and spherical.

Taking into account that the tray holes are 9 cm in diameter and the turbulence of liquid is very high Eq.9 were accepted.

$$C_D = 0.44 \qquad (9)$$

Substituting Eq. 9 in Eq. 8 gives the interfacial forces between liquid and gas phases.

$$M_{GL} = 0.33\frac{\alpha_G \rho_L}{d_G}|V_G - V_L|(V_G - V_L) \qquad (10)$$

The standard k-ε turbulence model has been used for simulating turbulence behavior of the liquid phase [10]. Turbulence model has not been used for the gas phase.

4. Flow geometry

The Concap tray used in the simulations is illustrated in Fig. 3(a) is a perspective of the tray. The proposed tray consists of 11 Concaps with holes of 9 cm in diameter at the tray deck and 4cm in diameter at the top of the cones.

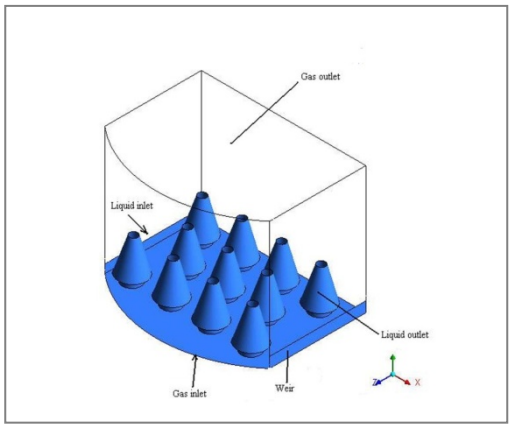

(a)

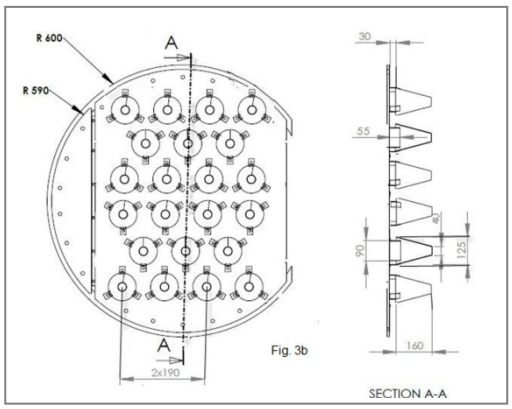

(b)

Figure 3: Flow geometry and boundary conditions of Concap tray in CFD simulation, (a) Tray prospective including Concaps, (b) Top and side views of Concap tray geometry.

Geometry arrangements and used dimensions are shown in Fig. 3(b) while riser height, angel and clearance of the cones are also indicated.

The effect of downcomers has been reported [11] but to reduce computer memory requirements and speed up calculations they were not included in the model geometry.

Additionally, due to the existence of a symmetry plane for the purpose of reduction of computational effort, only half of the tray was simulated. Plane z=0 is the plane of symmetry. As shown in Fig. 3(a) z-direction is normal to the flow direction (x-direction). Details of Concap and valve trays specifications which were used are given in Table 1. Tray geometry and operating conditions were based on the experimental works.

Table 1: Concap and valve tray specification

Characteristic	Concap tray	valve tray
Tower cross section diameter, m	1.22	1.22
Tray diameter, m	1.2	1.2
Tray spacing, mm	610	610
Weir height, mm	50	50
Weir length, mm	730	730
Downcomer clearance, mm	40	40
Hole diameter, mm	90	-
No. of holes	21	118
Tray thickness, mm	2	2
Riser height, mm	55	-
Hole area percentage	14%	14%
Active area, m^2	1.00776	1.00776

5. Boundary conditions

To solve the equations of continuity and momentum for the two-fluid mixture, appropriate boundary conditions for each phase should be specified at all internal and external boundaries of the simulated domain.

5.1. Liquid inlet

Eq. 11 gives the liquid inlet velocity profiles used in this work [3, 7, 11].

$$U_{L,in} = \frac{1.5Q_L}{A_{CL}}\left[1 - \left(\frac{2z}{L_W}\right)^2\right] \qquad (11)$$

Eq.11 is parabolic liquid inlet velocity profile. The liquid-volume fraction has been considered as unity at downcomer clearance because only liquid entered to the deck.

5.2. Vapor inlet

The gas inlet and outlet holes of the model have been individual cell faces at the bottom and top of the tray. The gas velocity at an inlet hole has been calculated such that the same mass flow rate enters through each hole [3].

$$V_{Air,in} = \left(\frac{V_S A_B}{2N_H}\right)\frac{1}{A_{Hole}} \quad (12)$$

Where, N_H is the number of holes in the model geometry (half of the full tray). The gas-volume fraction at the inlet holes has been specified to be unity.

5.3. Liquid and vapor outlets

The liquid- and vapor-outlet boundaries have been specified as mass flow boundaries with fractional mass flux specifications. At the liquid outlet, only liquid was assumed to leave the flow geometry while only gas could exit through the vapor outlet. These specifications have been in agreement with the specifications at the gas inlet and liquid inlet, where only one fluid was assumed to enter.

5.4. Wall

A no-slip wall boundary condition has been specified for the liquid phase and a free slip wall boundary condition was used for the gas phase.

At atmospheric pressure conditions, air and water have been used as the gas and liquid phases. The time step used in the simulations was 0.005 s. A transient simulation was assumed to be quasi- steady state if the value of clear-liquid height value remains constant with time. We achieved the steady state conditions in about 10 seconds from the start of the simulations, as shown in Fig. 4.

6. Results and Discussion

In our work CFD simulation results that were obtained for clear liquid height and total pressure drop were compared with the experimental data of Concap tray and valve tray in similar conditions. Liquid velocity distribution was obtained only with CFD because the experimental data of the horizontal liquid velocity distribution on the tray was not available. The CFD simulation and experimental works has been done in two liquid flow rates; Q_L=0.006 and 0.0122 m^3/s and four F-factors; F_S=1.44, 1.0, 0.79 and 0.47.

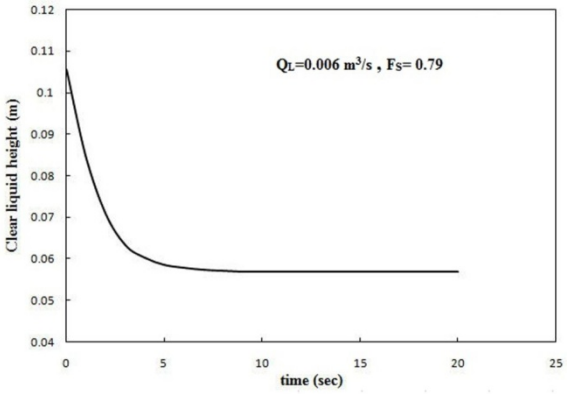

Figure 4: Quasi steady state approach based on the clear liquid height.

6.1. Velocity distribution

Solari and Bell [7, 3, 4], in their experimental work, have estimated the average velocity of the liquid by dividing the distance between two consecutive probes located in the same longitudinal row by the difference in mean residence time between the two probes.

In the present model similar to the Solari and Bell works the upstream and downstream profiles are defined for the Concap tray and are illustrated in Fig. 5.

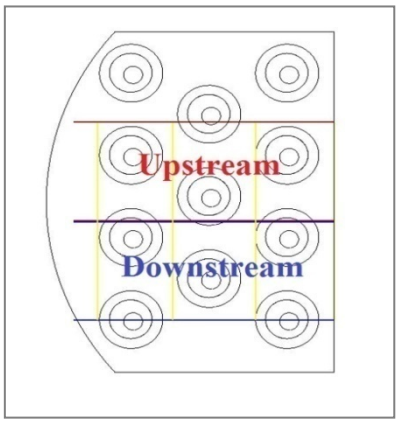

Figure 5: Up stream and downstream profiles defined for the Concap tray.

The horizontal liquid velocity distribution at the height of 4 cm above the tray deck has been measured by CFD analysis. The

average liquid velocity distribution in x-direction (Liquid U velocity) on Concap tray deck is predicted by the computational fluid dynamics.

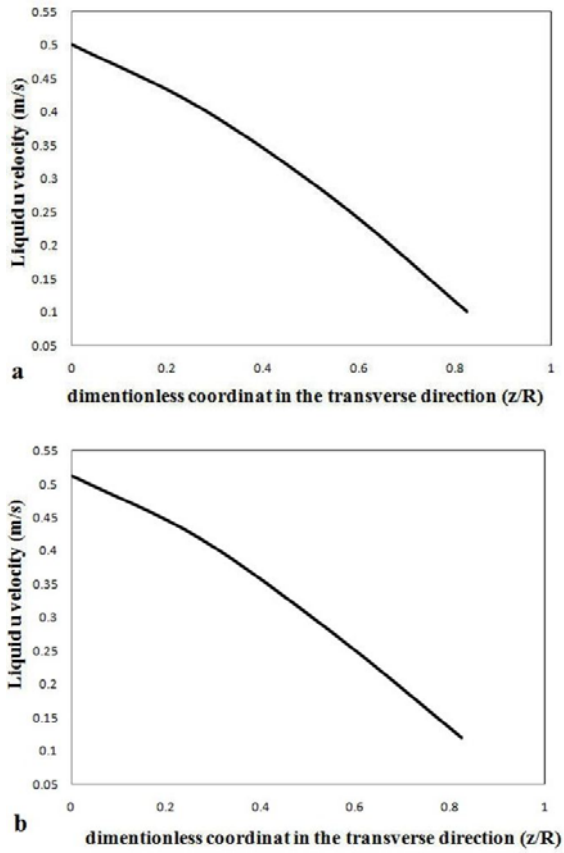

Figure 6: Liquid U velocity profile for QL= 0.0122 m3/s and Fs= 0.47 (a) Upstream profile (b) Downstream profile.

The results at different liquid and gas loads QL, F_s are given in the figures 6, 7, 8 and 9. Where, figures of type 'a' and type 'b' are for the up and for the down streams, respectively.

Because no experimental work has been done to determine those parameters, the accuracy of computational fluid dynamics results is not verified.

Variation of liquid velocity profiles for low Q_L= 0.006 m^3/s in traverse direction, as indicated in the Figs. 8 and 9, are higher than for higher Q_L= 0.0122 m^3/s in traverse direction, as indicated in the Figs. 6 and 7. As shown in these figures, the highest liquid velocity is in the center of the tray (z=0). As far away from the center of the tray, the liquid velocity was decreased. The lowest velocity was measured in the near of the tray wall. Therefore a non-uniform liquid distribution was observed in the Concap tray which is also observed in the common trays (sieve and valve trays) [2].

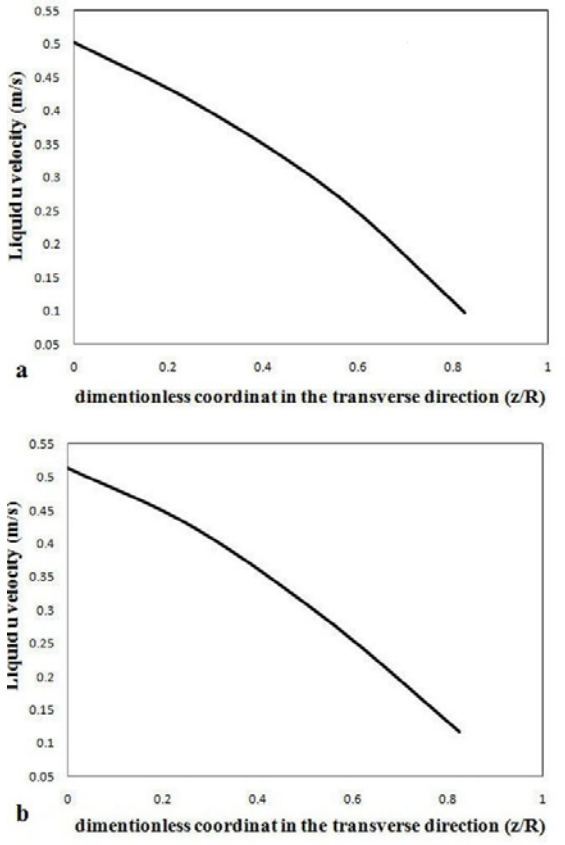

Figure 7: Liquid U velocity profile for QL= 0.0122 m3/s and Fs= 0.79 (a) Upstream profile (b) Downstream profile.

6.2. Pressure drop and clear liquid height

Clear liquid height and pressure drop on each tray is a criterion of performance and efficiency of the tray and is as a basic parameter for the investigation of hydrodynamics of the tray. Clear liquid height is a parameter which is used in the scale up of trays [2]. Figs. 10 and 11 are illustrations of variation of clear liquid height as function of F_s predicted by CFD simulations and experimental data at a constant liquid flow rate. From these figures it can be observed that with increasing the F_s the clear liquid height decreased. The agreement of computational fluid dynamics results of clear liquid height with experimental data for the Concap tray and valve tray were good as well.

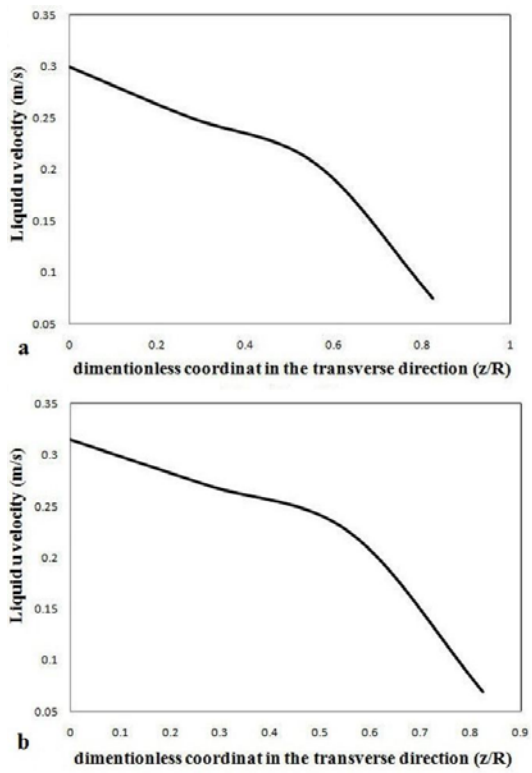

Figure 8: Liquid U velocity profile for QL= 0.006 m3/s and Fs= 1.0 (a) Upstream profile (b) Downstream profile.

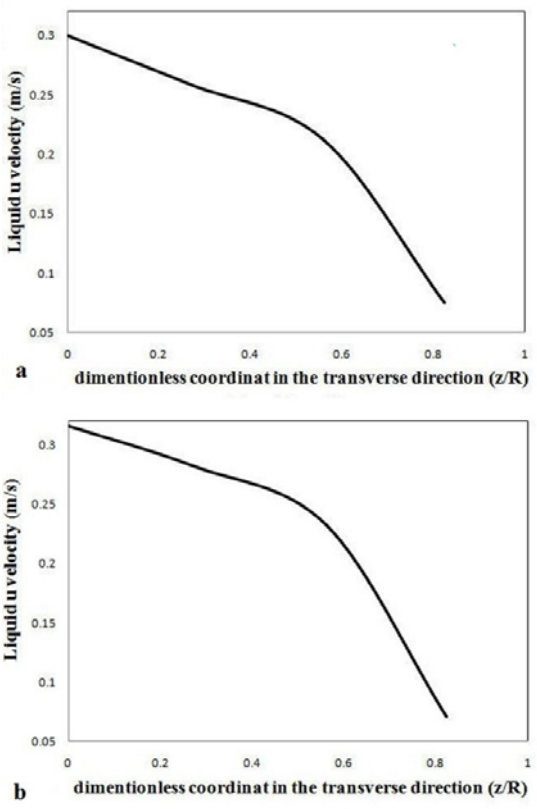

Figure 9: Liquid U velocity profile for QL= 0.006 m^3/s and Fs= 1.44 (a) Upstream profile (b) Downstream profile.

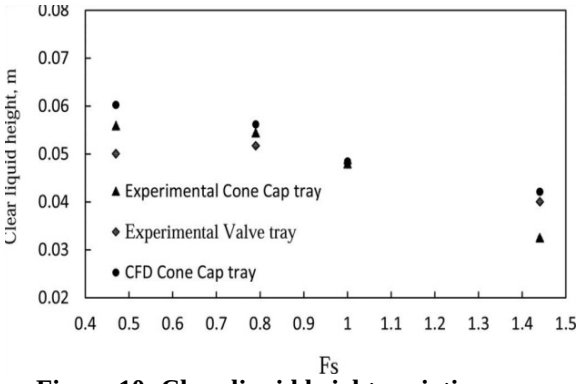

Figure 10: Clear liquid height variation as a function of Fs m/s(kg/m3)0.5 for constant liquid rate, QL= 0.006 m3/s.

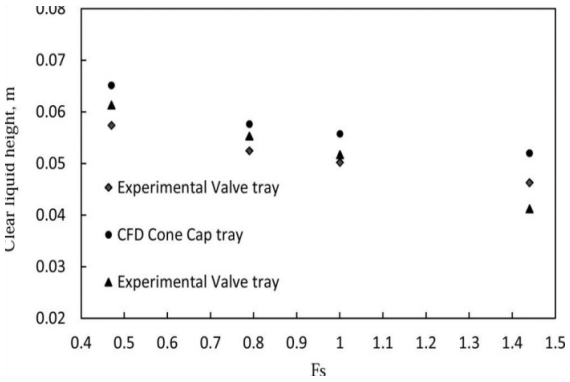

Figure 11: Clear liquid height variation as a function of Fs m/s(kg/m3)0.5 for constant liquid rate, QL= 0.0122 m3/s

Total pressure drop and clear liquid height of Concap tray was similar to valve tray having equal open holes area. From Fig. 12 and Fig. 13 it can be illustrated that the total pressure drop in the tray has been increased by increasing the gas flow rate at constant liquid flow rate.

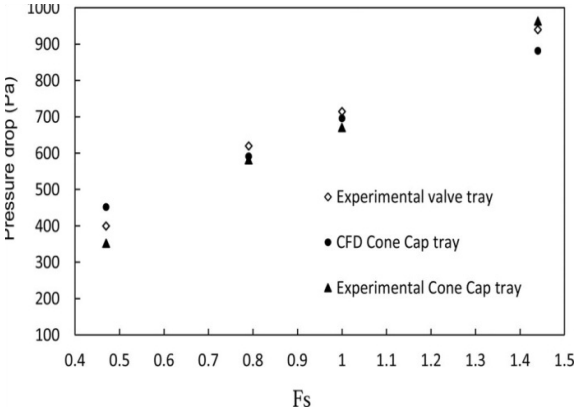

Figure 12: Total pressure drop variation as a function of Fs m/s(kg/m3)0.5 for constant liquid rate, QL= 0.006 m3/s.

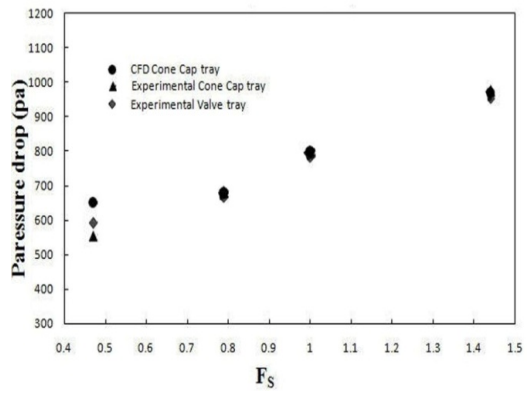

Figure 13: Total pressure drop variation as a function of Fs m/s(kg/m3)0.5 for constant liquid rate, QL= 0.0122 m3/s.

Fit of the data gave Equation 13 for variation of pressure drop, with gas and liquid flow rates.

$$\Delta P = 207.14F_s^2 - 1.87Q_L + 4.34Q_L \times F_s + 421.8 \quad R^2 = 0.97 \quad (13)$$

The computational fluid dynamics analysis for the pressure drop of Concap tray was in good agreement with the experimental data of Concap tray and is comparable with the valve tray pressure drop.

6.3. The Concap behavior

It has been mentioned that the performance of Concap tray is based on the variation of pressure that occurs inside a cone due to the gradual reduction in cross section and increasing of the gas velocity and reduction of the pressure within the cone. This pressure variation suctions the liquid into the cone and spray at outlet. The mechanism of Concap performance is clearly illustrated in Figs. 14 and 15.

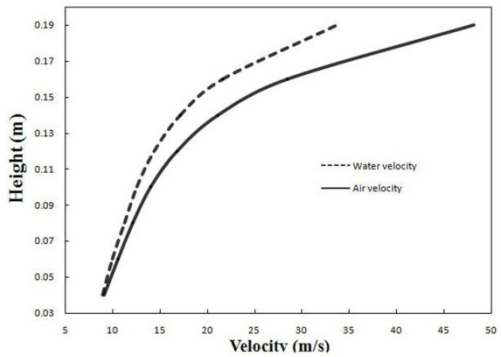

Figure 14: Variation of liquid and gas velocity within a cone as a function of height

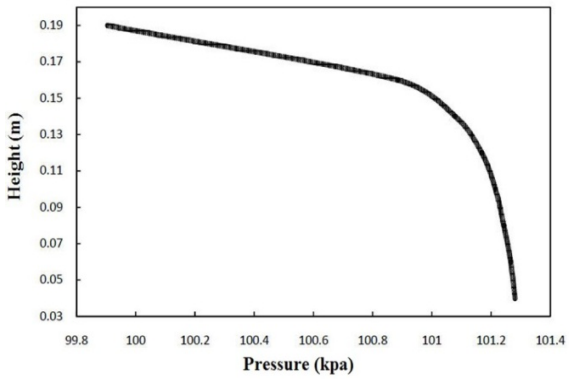

Figure 15: Variation of pressure within a cone as a function of height

Fig. 14 shows the variation of liquid and gas velocity within a cone as a function of cone height; whilst Fig. 15 is the illustration of the variation of pressure within that cone as a function of height. Fig. 14 shows that along the cone height the gas velocity has increased. The decrease of pressure along the cone height is given by Fig. 16. Variations of the velocity of water are shown in Fig. 14. According to these observations, it can be concluded that the air velocity is much more than water velocity inside the cone which results to spraying of some liquid droplets to the space above a Concap. These explanations are in agreement with the experimental observations.

6.4. Liquid distribution in the system

Fig. 16 is the illustration of contour plot of liquid volume fraction. Where, Figs. 17 and 18 are illustrations of liquid velocity vectors. Figs. 16 and 17 are for Concap tray at the plane (x-y) and at z = 0.095 m with F_S= 1.44 m/s$(kg/m^3)^{0.5}$ and Q_L=0.0122 m^3/s. Existence of sucked liquid into the Concap space is given by the liquid volume fraction. The suction of water by gas causes a high agitation of the liquid on the tray. This interaction causes more contact between the two phases upon the tray. At transient of two regions, there is no clear interface between gas and liquid phases. Fig. 18 illustrates the top view of liquid velocity vectors at 5 cm above the tray deck for Q_L=0.0122 m3/s and F_S=1.44 m/s $(kg/m^3)^{0.5}$. It can be observed that when

liquid enters the tray deck it passes by the Concaps and around the caps and the volumetric liquid fraction decreases. Liquid suction effects occur due to increase of gas velocity or pressure reduction, leaving the Concaps. Whilst this pressure drop could be explained by energy equations, the drag coefficients require further studies.The reduction of pressure is also indicated by Fig.18. From this figure it can be observed that liquid is suctioned into the cones.

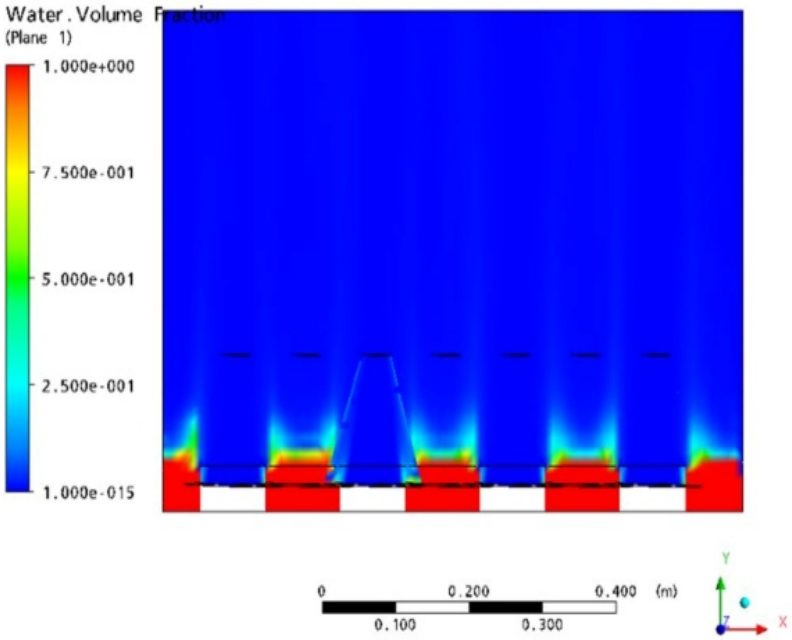

Figure 16: Contour plot of liquid volume fraction on a xy face at z= 0.095m from the tray center. QL=0.0122 m3/s, FS=1.44 m/s (kg/m3)0. 5.

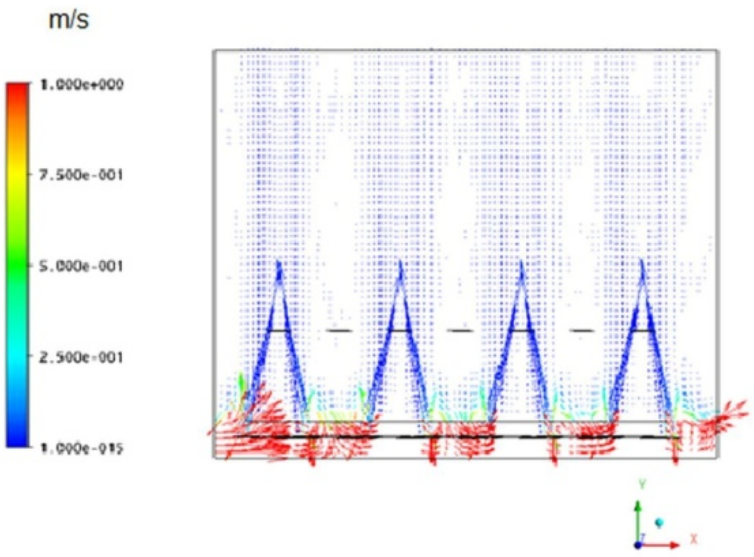

Figure 17: Liquid velocity vectors on a xy plane atz= 0.095m from the tray center. QL=0.0122 m3/s, FS=1.44 m/s (kg/m3)0. 5.

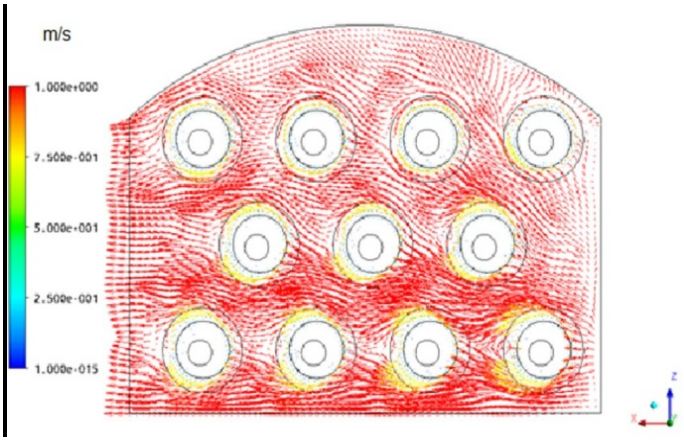

Figure 18: Liquid velocity vectors at 5cm above the tray deck. QL=0.0122 m3/s, FS=1.44 m/s(kg/m3)0. 5.

From Figs. 16, 17 and 18 it can be concluded that the turbulence of liquid around of holes is high while the chaotic behavior can be realized from the velocity vector plots. In these experiments, the effect of riser height has not been considered but it has been realized that for conduction passage of the gas through the cone it cannot be removed.

7. Conclusions

In this study a transient three-dimensional and two-phase computational fluid dynamics model has been presented to simulate hydraulic of a Concap tray. The CFD model was developed in the Eulerian-Eulerian framework. The Concap tray modeling has investigated in an air-water system based on operating conditions of experimental works for a 1.2 m in diameter Concap tray. The results of the modeling with computational fluid dynamics have been compared with the experimental data of Concap tray and valve tray. The gas and liquid phase equations were coupled through an interphase momentum transfer term that was estimated locally using the constant drag coefficient equal to 0.44.

The horizontal velocity distribution of liquid on the tray was investigated with computational fluid dynamics only،due to the lack of the experimental data, velocity profiles have been reported. The total pressure drop and clear liquid height on Concap tray has been measured. The simulation results exhibit some known features of the two-phase flow field in Concap trays and are in good agreement with the experimental results. It has been found that the pressure drop and the clear liquid height of the Concap tray are similar to valve tray at the same operating conditions. Experimental data are scarce, so extensive research efforts should be dedicated to provide experimental data suitable for validation of more complex trays than sieve or valve trays. Similarity criteria should be redefined for the purpose of scale up. Tray dimension requires optimizations.

▪ Acknowledgement

Authors would like to give their appreciation to Azar Energy Company for providing facilities for the construction and experimentation with the Concap tray.

▪ Nomenclature

A_B	m^2	tray bubbling area
A_{CL}	m^2	liquid clearance area
A_{Hole}	m^2	Area of a hole
C_D		drag coefficient
d_G	m	mean bubble diameter
F_S		F-factor=$V_S\sqrt{\rho_G}$
g	m/s^2	gravity acceleration
L_W	m	inlet weir length
M_{GL}	$kg.m^{-2}.S^{-2}$	interphase momentum transfer
P_G	$N.m^{-2}$	gas phase pressure

P_L	N.m^{-2}	Liquid phase pressure			
Q_L	m^3/s	liquid volumetric flow rate	z	m	coordinate position in the transverse direction to liquid flow across tray
$U_{L,in}$	m/s	x-component of liquid velocity at the inlet boundary condition	***Greek symbols***		
V_G	m/s	gas phase velocity vector	α_G		volume fraction of gas
V_L	m/s	liquid phase velocity vector	α_L		volume fraction of liquid
V_S	m/s	gas phase superficial velocity based on the bubbling area	ΔP		Tray Pressure drop (Pa)
			$\mu_{eff,G}$	kg·m^{-1}·s^{-1}	effective viscosity of gas
x	m	coordinate position in the direction of liquid flow across tray	$\mu_{eff,G}$	kg·m^{-1}·s^{-1}	effective viscosity of liquid
y	m	coordinate position in the direction of vapor flow across tray	ρ_G	kg.m^{-3}	density of gas
			ρ_L	kg.m^{-3}	density of liquid
			ε	W kg^{-1}	dissipation rate of k

References:

1–Wesselingh, J.A. and Krishna, R. (2000). *Mass Transfer in Multicomponent Mixtures.* Delft University Press.

2– Kister, H.Z. (1992). *Distillation Design*. McGraw-Hill, New York.

3– Gesit, G., Nandakumar, K. and Chuang, K.T. (2003). "CFD modeling of flow patterns and hydraulics of commercial-scale sieve trays." *AIChE J.*, Vol. 49, pp.910–924.

4– Solari, R.B. and Bell, R.L. (1986). "Fluid Flow Patterns and Velocity Distribution on Commercial-Scale Sieve Trays." *AIChE J.*, Vol. 32, pp. 640-649.

5– Rahimi, R., Rahimi, M.R., Shahraki, F. and Zivdar, M. (2006). "Efficiencies of sieve tray distillation columns by CFD simulations."*Chem. Eng. Technol*., Vol. 29, No. 3, pp. 326-335.

6– Li, X.G., Liu, D. X., Xu, S. M. and Li, H. (2009). "CFD simulation of hydrodynamics of valve tray." *Chem.l Eng. Process.: Process Intensification*, Vol. 48, pp. 145-151.

7– Zarei, T., Rahimi, R. and Zivdar, M. **(**2009). "Computational fluid dynamic simulation of MVG tray hydraulics."*Korean J. Chem. Eng*., Vol.26, No. 5, pp. 1213-1219.

8– Zarei, A., Rahimi, R., Zarei, T. and Naziri, N. (2010) "A study on sieve tray lower operating limit" *Distillation Absorption conference, Netherland, Eindhoven*, pp. 479-484.

9– Fischer, C.H. and Quarini, J.L. (1998) "Three-dimensional heterogeneous modeling of distillation tray hydraulics." *AIChE Meeting, Miami Beach, FL*

10– CFX User Manual, ANSYS, Inc. Modeling, CFX 11.0: Solver.

11– Rahimi, R., Ameri, A. and Setoodeh, N. (2011). "Effect of Inlet Downcomer on the Hydrodynamic Parameters of Sieve Trays Using CFD Analysis."*J. Chem. Petrol. Eng.*, Vol. 45, No. 1, pp. 27- 38.